Maximum Power-Point Extraction of Small Switched-Inductor Piezoelectric Harvesters

Jun-Yang Lei, *Graduate Student Member, IEEE,* and Gabriel A. Rincón-Mora*, Fellow, IEEE*
Georgia Institute of Technology, Atlanta, Georgia 30332 U.S.A.
E-mail: clei8@gatech.edu and Rincon-Mora@gatech.edu.

***Abstract*—Piezoelectric harvesters are popular today because they typically draw more power from kinetic energy in motion than electrostatic and electromagnetic systems. Still, tiny transducers only derive a small fraction of what is available. Thankfully, raising the damping force with which transducers draw power increases that fraction, except overinvesting battery energy for that purpose can overdamp the system. This is why harvesters monitor output power, and current, which normally requires fast and accurate circuits that consume substantial power. This paper, however, presents a low-loss alternative. The idea is to sense how output power changes by monitoring the time that the switched inductor requires to drain its energy. This way, with readily available parameters, a piezoelectric harvester can estimate the investment that will keep the system within 2.5% of its maximum power point.**

Keywords—Piezoelectric transducer, harvester, ambient kinetic energy, motion, maximum power point, switched inductor.

I. Harvesting Energy from Tiny Tansducers

Wireless microsensors can add performance-enhancing and energy-saving intelligence to many inaccessible and difficult-to-reach places, like hospitals, factories, farms, and others [1]–[2]. Unfortunately, the tiny batteries that these systems can afford to incorporate cannot sustain life over extended periods, which is what many applications demand. Harvesting energy from the surrounding environment, however, can.

Of available ambient sources, kinetic energy in motion is popular because vibrations in cars, airplanes, and motors are abundant and steady [3]–[4]. Piezoelectric harvesters lead the charge in this regard because they normally generate more power than their electrostatic and electromagnetic counterparts [3]. But since the damping force that miniaturized transducers impose on vibrations is miniscule, output power is very low. This is why state-of-the-art harvesters use battery energy to raise the electrical damping force in the transducer, because a higher damping force draws more power from motion [5].

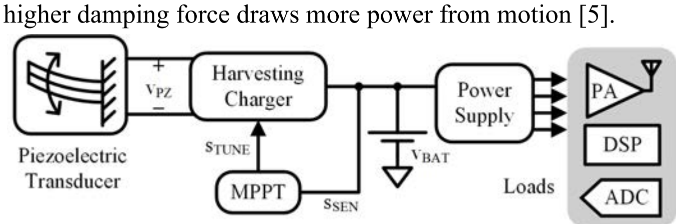

Fig. 1. Typical piezoelectric energy-harvesting microsystem.

Overdamping the system, however, is possible. If this happens, a higher damping force causes more losses than gains. Piezoelectric harvesters must therefore monitor variations in output power, and adjust accordingly to ensure the systems remain near their maximum power point (MPP). But since vibrations are often intermittent, and tiny transducers generate little power, microsystems normally use a harvesting charger to replenish a small on-board battery. This way, a power-supply circuit like the one Fig. 1 illustrates can draw from the battery (at any time) the power that the system requires.

Monitoring how output power changes without introducing a lossy sensor into the conduction path, or without requiring precision circuits that consume considerable power, is challenging. This paper, however, shows how energy-investing switched-inductor piezoelectric harvesters can monitor variations in power from connection times that are readily available. Before introducing the scheme, though, Section II first explains the importance and operation of a switched inductor in piezoelectric chargers. Section III then describes how to monitor variations in output power from the time that this inductor requires to drain its energy. Sections IV, V, and VI finish by showing, discussing, and concluding how well this metric is able to track the maximum power point of the system.

II. Piezoeletric Chargers

A. The State of the Art

Since piezoelectric transducers generate alternating currents that produce ac voltages and batteries establish static dc voltages, many harvesters in literature use bridge rectifiers [6]–[8]. These ac–dc converters output charge when the piezoelectric voltage v_{PZ} rises above the rectified output v_{REC}. Output power is highest when the voltage drops across the switches in the network are nearly negligible [7] and v_{REC} is half the amplitude of v_{PZ}'s open-circuit voltage $v_{PZ(OC)}$ [8].

Unfortunately, conventional bridge rectifiers suffer from two significant drawbacks. First, when operating at their maximum power point, they only collect half of the charge generated. And for this, v_{REC} should be $0.5v_{PZ(OC)}$. But since the battery voltage v_{BAT} is not controllable, a regulating dc–dc converter must buffer the bridge from v_{BAT}. In other words, these harvesters also require an intermediate dc–dc converter.

To overcome the first limitation, the bridge rectifier in [9] transfers the uncollected charge in the piezoelectric capacitance C_{PZ} at the end of every half cycle into an inductor that pumps it immediately back into C_{PZ}. As a result, C_{PZ} quickly discharges to ground and charges to v_{REC} in the opposite direction. Since v_{PZ} is almost always at v_{REC}, except briefly between half cycles, the system collects nearly all the charge generated.

The switched inductor in [10] overcomes the second limitation. For this, [10] lets C_{PZ} accumulate all the charge that motion generates across every half cycle. Then, between half cycles, the system discharges C_{PZ} into an inductor that then drains the inductor into v_{BAT}. This way, without an intervening dc–dc converter, all the charge generated reaches v_{BAT}.

Still, tiny transducers only capture a miniscule fraction of the energy that is available, so output power is nevertheless low. This is why the switched inductor in [11] invests battery energy into C_{PZ}, to raise the electrostatic force with which C_{PZ} draws power from motion. Since C_{PZ} collects charge at a higher voltage, C_{PZ} draws more energy from motion. If v_{PZ} is too high, though, C_{PZ} can overdamp vibrations to the extent that output power falls. Or if the battery investment is excessive, ohmic losses can be high enough to nullify gains. To avoid these unfavorable conditions, [11] should (but does not) monitor and track its maximum power point.

B. Energy-Investing Switched-Inductor Charger

Figure 2 illustrates the energy-investing switched-inductor piezoelectric harvester in [11]. Leakage through the transducer is normally so low that R_{PZ} hardly affects the circuit. So with zero volts to start and both switches open, C_{PZ} first collects all the charge that motion generates with i_{PZ} across its positive half cycle. v_{PZ} in Fig. 3 therefore rises and peaks to $v_{PZ(PK+)}$ at 2 ms.

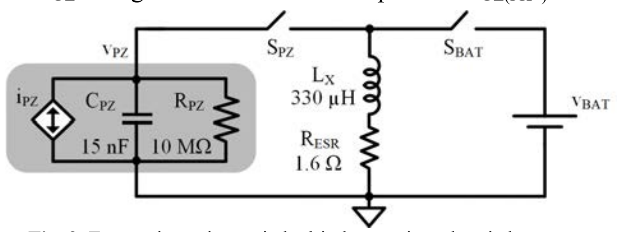

Fig. 2. Energy-investing switched-inductor piezoelectric harvester.

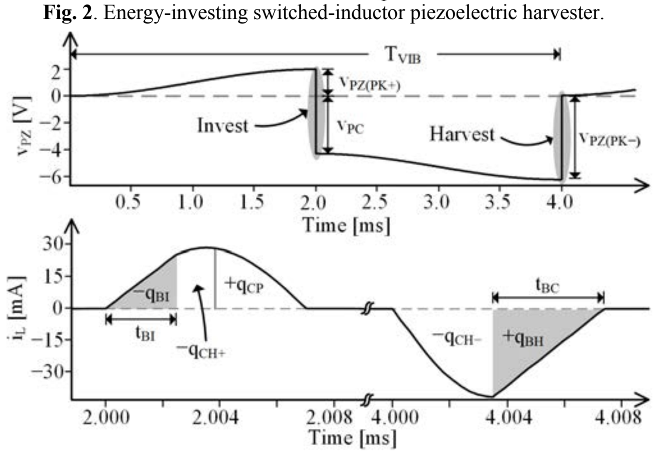

Fig. 3. Simulated time-domain waveforms.

At that point, at 2 ms, switch S_{BAT} closes to deposit battery energy into the inductor L_X. L_X's current i_L therefore rises, and after t_{BI}, reaches 26 mA. Then, S_{BAT} opens and S_{PZ} closes to drain C_{PZ} into L_X. So as v_{PZ} falls to ground, i_L rises more to peak at 29 mA. But with S_{PZ} still closed, L_X drains into C_{PZ} in resonance fashion and C_{PZ} charges in the opposite direction to $-v_{PC}$. S_{PZ} opens when L_X depletes to keep C_{PZ} from draining back into L_X. In all, L_X recycles C_{PZ}'s energy and invests v_{BAT}'s energy into C_{PZ} in about 7 µs of the 4-ms period T_{VIB}.

With both switches open, i_{PZ} deposits charge into C_{PZ} across i_{PZ}'s negative half cycle. As a result, C_{PZ} charges further in the negative direction, from $-v_{PC}$ at 2 ms to $-v_{PZ(PK-)}$ at 4 ms. After this, in about 7.5 µs, S_{PZ} first closes to drain C_{PZ} into L_X and then S_{PZ} opens and S_{BAT} closes to deplete L_X into v_{BAT}. After this, another vibration cycle begins.

C. Maximum Power Point

The system overdamps motion when the electrostatic field across C_{PZ} couples an impeding mechinal force that is large enough to surpass the force vibrations produce in the first place [12]–[13]. But since the electromechanical coupling factor k_C of tiny devices is very low, the effects on motion are almost negligible. So when neglecting the effects of other factors, output power P_O climbs monotonically with the damping forces that increasing levels of investment energy produce.

Another possible limitation is the breakdown voltage of the chip. But with a high-voltage technology, power losses in the system subtract and limit to what extent P_O can rise. The reason for this is, switches and the series resistance of the inductor dissipate more ohmic power P_{LOSS} when they conduct more energy. In the case of the energy-investing system, extending the investment time t_{BI} that v_{BAT} requires to deposit energy into L_X raises the power that v_{BAT} delivers, the damping force that C_{PZ} establishes, and in consequence, the power P_{IN} that C_{PZ} draws from i_{PZ}. So with more power flowing through the system, P_{LOSS} in Fig. 4 rises with t_{BI}.

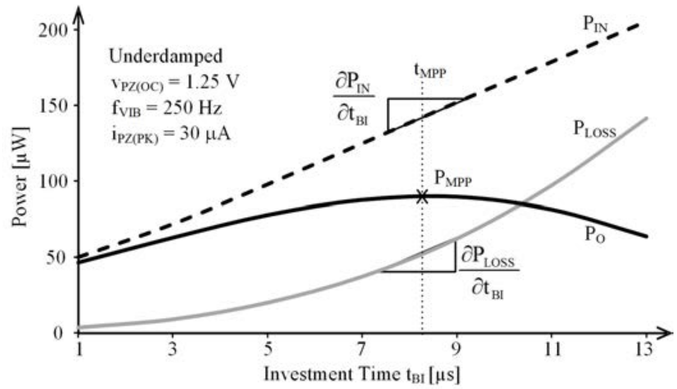

Fig. 4. Simulated input, output, and lost power across investing level.

In fact, with higher investment levels, input power P_{IN} increases linearly and ohmic losses P_{LOSS} quadratically [11]. This is unfortunate because the rise in P_{LOSS} at some point cancels that of P_{IN}. Beyond this maximum power point P_{MPP}, P_O drops with higher investments. In other words, the system begins to overdamp after the rise in P_{LOSS} matches that of P_{IN}:

$$\left.\frac{\partial P_{IN}}{\partial t_{BI}}\right|_{P_O=P_{MPP}} = \frac{\partial P_{LOSS}}{\partial t_{BI}} . \quad (1)$$

t_{BI} should therefore be at the setting that balances this tradeoff, which is when the system outputs maximum power P_{MPP}.

III. Maximum Power-Point Extraction

To track the maximum power point P_{MPP}, the system must monitor how output power P_O changes with the tuning variable s_{TUNE} in Fig. 1, or in the switched-inductor case of Fig. 2, with investment time t_{BI}. Luckily, vibrations in cars, planes, boats, and other places are steady, so P_{MPP} hardly changes across cycles. The system can therefore take several cycles to sense P_O and adjust and lock t_{BI} so P_O is near P_{MPP}.

The popular hill-climbing algorithm [14], in fact, relies on this slow time constant. With this scheme, the system raises s_{TUNE} in one cycle and monitors how P_O responds in the next. If P_O rises, the system again raises s_{TUNE}, and continues this way after each consecutive cycle until P_O finally drops. When P_O falls, which happens only after t_{BI} in Fig. 4 increments past its optimal setting t_{MPP}, the system locks or alternates between the last two settings. Since the small deviation in t_{BI} that results from switching between consecutive settings near t_{MPP} causes minimal variations in P_O, P_O remains near P_{MPP}.

A. Sense Output Power

Output power P_O is the product of battery voltage v_{BAT} and the current that v_{BAT} receives as i_{BAT}. Unfortunately, sensing i_{BAT} by monitoring the voltage v_S that a series resistor R_S drops requires substantial power. If R_S is one of the switches in the network, for example, v_S is low and changes quickly. This means, the circuit used to monitor v_S must be accurate and fast, and as a result, also lossy [15]. Even if R_S is not already in the circuit, adding R_S raises ohmic losses P_{LOSS} in the circuit, so R_S and v_S should also be low. A low-pass filter across the inductor also produces a voltage that is proportional to i_{BAT}. Except, the voltage is low, sensing circuits are complex, and the filter is bulky (and normally off chip) [15].

B. Extract Output Power from Connection Times

Monitoring how much energy inductor L_X transfers is another way of sensing power. L_X's current i_L is key in this respect because i_L determines how much energy L_X holds as E_L or $0.5L_Xi_L^2$. Luckily, L_X's voltage v_L is nearly constant through every transaction, so time t_X sets i_L to t_Xv_L/L_X and E_L to

$$E_L = 0.5L_Xi_L{}^2 = 0.5L_X\left[\left(\frac{v_L}{L_X}\right)t_X\right]^2 = \left(\frac{v_L{}^2}{2L_X}\right)t_X{}^2. \qquad (2)$$

In other words, connection time can be an indicator for power.

In the case of the energy-investing switched-inductor piezoelectric harvester in Fig. 2, v_{BAT} collects energy E_{BC} when L_X connects to v_{BAT} across collection time t_{BC} at the end of the negative half cycle (from Fig. 3). Similarly, v_{BAT} invests energy E_{BI} when L_X connects to v_{BAT} across investment time t_{BI} at the end of the positive half cycle. Output energy per cycle E_O is therefore their difference:

$$E_O = E_{BC} - E_{BI} = \left(\frac{v_{BAT}{}^2}{2L_X}\right)\left(t_{BC}{}^2 - t_{BI}{}^2\right) \propto t_{BC}{}^2 - t_{BI}{}^2, \qquad (3)$$

where v_L is v_{BAT}, P_O is E_O over the vibration period T_{VIB}, and P_O and E_O are both proportional to $t_{BC}{}^2 - t_{BI}{}^2$.

IV. PERFORMANCE

A. Error

In practice, v_L is not exactly v_{BAT} across collection time t_{BC} or investment time t_{BI}. The reason for this is that parasitic resistances R_{ESR} in the conduction path drop part of v_{BAT}. Or stated differently, R_{ESR} consumes some of the energy that v_{BAT} would have otherwise invested or collected.

Luckily, R_{ESR} is so low that it drops a small fraction of v_{BAT}. 1.6 Ω, for example, causes a 0.9-mA or 1.2% error in the 73.4 mA that i_L builds over the 7-µs span that v_{BAT} requires to invest E_{BI} in Fig. 5. Since the estimated current i_L' neglects the energy lost in R_{ESR}, i_L is lower than i_L'. In other words, this method overestimates the investment E_{BI}.

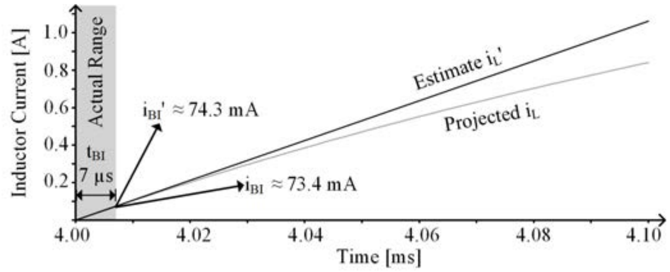

Fig. 5. Simulated and predicted investment current through the inductor.

Similarly, 1.6 Ω in Fig. 6 causes a 2-mA or 2.2% error in the 88.7 mA that L_X holds when L_X starts draining E_{BC} into v_{BAT}, which requires 8.18 µs to exhaust. Since the estimate i_L' neglects the loss in R_{ESR}, L_X delivers more energy than predicted by t_{BC}. i_L is therefore higher than i_L', and v_{BAT} receives more charge than expected.

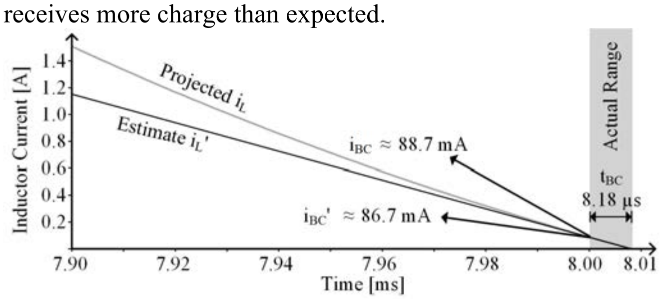

Fig. 6. Simulated and predicted collection current through the inductor.

B. Output Power

Because overestimating the investment and underestimating the collection are both pessimistic, P_O in Fig. 7 is higher than predicted. In fact, since R_{ESR} consumes more power when L_X transfers more energy, errors in i_L climb with higher power levels. Figures 5 and 6 show this because, with more energy, L_X requires more time to energize and drain. And with more time, the error between i_L' and i_L grows. This is why the difference between P_O and P_{EST} swells with rising investments.

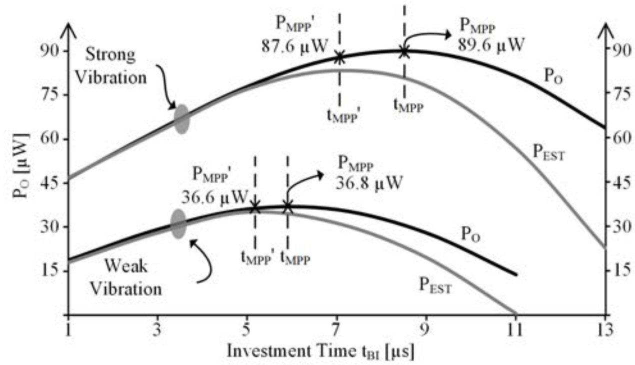

Fig. 7. Simulated and predicted output power across investment time.

C. Maximum Power Point

Since the error worsens with rising power levels, the prediction is more accurate with lower investments. In fact, the error near the maximum power point P_{MPP} is not significant, as Fig. 7 demonstrates. As a result, the predicted maximum power point

P_{MPP}' is only 2 μW below the 89.6 μW peak that 30 μA of piezoelectric current i_{PZ} across 15 nF can produce and 0.2 μW below the 36.8 μW that 17.5 μA across 15 nF can generate.

Interestingly, the optimal investment time predicted t_{MPP}' is consistently lower than the actual counterpart t_{MPP}. This happens because the prediction is invariably pessimistic, and the error nevel fails to climb with higher investment levels. In other words, the prediction overestimates how fast losses grow. With vibrations that produce 30 μA, for example, the predicted investment time t_{MPP}' is roughly 7 μs, whereas the actual t_{MPP} is 9 μs. Similarly, t_{MPP}' for 17.5 μA is 5 μs and t_{MPP} is 6 μs.

As Fig. 7 shows, however, output power P_O hardly changes near its maximum power point P_{MPP}. This means, a slight deviation from the optimal investment time produces a small error in the maximum power point. This is why the maximum power-point error $\Delta P_{MPP(E)}$ in Fig. 8 is below 2.5% for vibrations that produce up to 89.7 μW from up to 30 μA of piezoelectric current across 15 nF. Since the prediction is increasingly pessimistic with higher power levels, the error is less than 1% for up to 15 μA and 1.5%–2.5% for 16–30 μA.

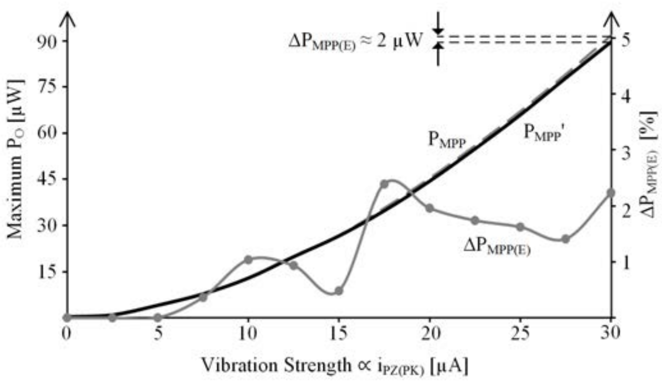

Fig. 8. Maximum output power and power point error across vibration strength.

V. Implementation

Ultimately, knowing P_O or E_O is not important when hill-climbing towards P_{MPP}. What matters is how P_O or E_O changes across cycles. And since both P_O and E_O are proportional to $t_{BC}^2 - t_{BI}^2$, variations in this difference is sufficient to find the optimal investment time t_{MPP} with which the system produces the most output power P_{MPP}. In other words, removing $v_{BAT}^2/2L_X$ and T_{VIB} from E_O's and P_O's expressions does not change the behavior or location of the peak in Fig. 7. This means, knowing the values of v_{BAT}, L_X, and T_{VIB} is entirely unnecessary when finding t_{MPP}'.

Since the tuning variable s_{TUNE} in Fig. 1 with which the harvester in Fig. 2 adjusts is the investment time t_{BI} in Fig. 3, t_{BI} is a known quantity. The only "unknown" in $t_{BC}^2 - t_{BI}^2$ is the collection time t_{BC}. But since the controller that switches L_X in Fig. 2 sets t_{BC}, t_{BC} is also known. So with t_{BC} and t_{BI}, the controller can decipher t_{MPP}'. And since t_{MPP}' always lags t_{MPP}, the system can also offset the prediction to reduce the error.

VI. Conclusions

The algorithm presented here can find the maximum power point of small energy-investing switched-inductor piezoelectric harvesters without sensing current, and with less than 2.5% error. The system therefore saves the power that a calibration period or a current sensor would have otherwise required. This savings is significant because skipped cycles and circuits that sense current lose considerable power. True, typical bridge rectifiers do not use an inductor. However, switching an inductor not only avoids the overhead of a charging dc–dc buffer but also allows the system to raise the damping force in the transducer. This is important because small transducers suffer from low electromechanical coupling factors. So without energy with which to raise the damping force in the transducer, output power is very low. In other words, switching an inductor as proposed outputs the highest possible power.

Acknowledgement

The authors thank Kowshik Murali for his contributions.

References

[1] R.J.M. Vullers, R.V. Schaijk, H.J. Visser, J. Penders, and C.V. Hoof, "Energy harvesting for autonomous wireless sensor networks," *IEEE Solid-State Circuits Magazine*, vol. 2, no. 2, pp. 29–38, Spring 2010.

[2] D.A. La Van, T. McGuire, and R. Langer, "Small-scale systems for in vivo drug delivery," *Nature Biotechnology*, vol. 21, no. 10, pp. 1184–1191, Oct. 2003.

[3] S. Roundy, P.K. Wright, and J. Rabaey, "A study of low level vibrations as a power source for wireless sensor nodes," *Computer Communications*, vol. 26, no. 11, pp. 1131–1144, 1 July 2003.

[4] P.D. Mitcheson, E.M. Yeatman, G.K. Rao, A.S. Holmes, and T.C. Green, "Energy harvesting from human and machine motion for wireless electronic devices," *Proceedings of the IEEE*, vol. 96, no. 9, pp. 1457–1486, Sept. 2008.

[5] R.D. Prabha, D. Kwon, O. Lazaro, K.D. Peterson, and G.A. Rincón-Mora, "Increasing electrical damping in energy-harnessing transducers," *IEEE Transactions on Circuits and Systems II*, vol. 58, no. 12, pp. 787–791, Dec. 2011.

[6] G.A Lesieutre, G.K Ottman, and H.F. Hofmann, "Damping as a result of piezoelectric energy harvesting," *Journal of Sound and Vibration*, v. 269, n. 3-5, pp. 991–1001, Jan. 2004.

[7] Y. Lam, W. Ki, and C. Tsui, "Integrated low-loss CMOS active rectifier for wirelessly powered devices," *IEEE Transactions on Circuits and Systems II*, vol. 53, no. 12, pp.1378–1382, Dec. 2006.

[8] G.K. Ottman, H.F. Hofmann, A.C. Bhatt, and G.A. Lesieutre, "Adaptive piezoelectric energy harvesting circuit for wireless remote power supply," *IEEE Transactions on Power Electronics*, vol. 17, no. 5, pp. 669–676, Sept. 2002.

[9] Y.K. Ramadass and A.P. Chandrakasan, "An efficient piezoelectric energy harvesting interface circuit using a bias-flip rectifier and shared inductor," *IEEE Journal of Solid-State Circuits*, vol. 45, no. 1, pp. 189–204, Jan. 2010.

[10] D. Kwon and G.A. Rincón-Mora, "A single-inductor ac–dc piezoelectric energy-harvester/battery-charger IC converting ±(0.35 to 1.2V) to (2.7 to 4.5V)," *IEEE Int. Solid-State Circuits Conf.*, pp. 494–495, Feb. 2010.

[11] D. Kwon and G.A. Rincón-Mora, "A single-inductor 0.35μm CMOS energy-investing piezoelectric harvester," *IEEE Int. Solid-State Circuits Conf.*, pp. 78–79, Feb. 2013.

[12] P.D. Mitcheson, T.C. Green, E.M. Yeatman, and A.S. Holmes, "Architectures for vibration-driven micropower generators," *J. of Microelectromechanical Systems*, vol. 13, no. 3, pp. 429–440, June 2004.

[13] D. Galayko and P. Basset, "A general analytical tool for the design of vibration energy harvesters (VEHs) based on the mechanical impedance concept," *IEEE Transactions on Circuits and Systems I*, vol. 58, no. 2, pp. 299–3311. Feb. 2011.

[14] T. Esram and P.L. Chapman, "Comparison of photovoltaic array maximum power point tracking techniques," *IEEE Transactions on Energy Conversion*, vol. 22, no. 2, pp. 439–449, June 2007.

[15] H.P. Forghani-zadeh and G.A. Rincón-Mora, "Current-sensing techniques for dc–dc converters," *IEEE Midwest Symposium on Circuits and Systems*, vol. 2, pp. 577–580, Aug. 2002.